

# Summary of NSLS-II Source Properties

## User Workshop July 17-18, 2007

This handout provides a summary of some of the current NSLS-II source parameters. For a more complete description of the radiation sources planned for NSLS-II, see Chapter 8 of the NSLS-II Conceptual Design Report [<http://www.bnl.gov/nsls2/project/CDR/>]. We note that this document summarizes the present status of the design, but that the design continues to be refined and that these parameters may change as part of this process.

NSLS-II is designed to deliver photons with average spectral brightness in the 2 keV to 10 keV energy range exceeding  $10^{21}$  ph/mm<sup>2</sup>/mrad<sup>2</sup>/s/0.1%BW. The spectral flux density should exceed  $10^{15}$  ph/s/0.1%BW in all spectral ranges. This cutting-edge performance requires the storage ring to support a very high-current electron beam ( $I = 500$  mA) with sub-nm-rad horizontal emittance (down to 0.5 nm-rad) and diffraction-limited vertical emittance at a wavelength of 1 Å (vertical emittance of 8 pm-rad). The electron beam will be stable in its position (<10% of its size), angle (<10% of its divergence), dimensions (<10%), and intensity ( $\pm 0.5\%$  variation). The latter requirement provides for constant thermal load on the beamline front ends.

The optimized storage ring lattice consists of 30 DBA cells, with straight sections alternating in length between 6.6 m and 8.6 m, with low and high values of horizontal beta functions, respectively. All of the source properties described in this handout assume a fully-damped horizontal emittance of 0.55 nm-rad. This is the performance goal for the NSLS-II storage ring when operating with a full complement of eight 7 m damping wigglers. The initial horizontal emittance of 0.9 nm-rad will be somewhat larger than this, due to the fact that only three 7 m damping wigglers will be installed at the start of operations. The main parameters of the storage ring are summarized in Table 1.

The one sigma horizontal and vertical electron beam sizes and divergences in the center of the two types of straights, at the planned location of the 3-pole wigglers, and the range of values in the bend magnets, are given in Table 2. For comparison, the corresponding electron beam size and divergence values for NSLS x-ray ring sources are given in Table 3.

Continuing the tradition established by the NSLS, the NSLS-II radiation sources span a very wide spectral range, from the far IR, down to 0.1 meV (equivalent to  $1 \text{ cm}^{-1}$ ), to the very hard x-ray region, more than 300 keV. This is achieved by a combination of bending magnet sources (both standard gap and large gap), covering the IR, VUV, and soft x-ray range, three-pole wigglers, covering the hard x-ray range up to  $\sim 20$  keV, and insertion device sources (undulators, damping wigglers, and superconducting wigglers), covering the VUV through the very hard x-ray range.

The basic parameters characterizing the NSLS-II IDs and bending magnet sources are listed in Table 4. Here, SCU stands for superconducting undulator, CPMU for cryogenic, permanent magnet undulator, EPU for elliptically polarized undulator, PMW for permanent magnet wiggler, SCW for superconducting wiggler, and 3PW for three pole wiggler. All parameters are for 3.0 GeV, 500 mA operations.

**Table 1. Main Parameters of the NSLS-II Storage Ring.**

Energy [GeV]	3
Circumference [m]	791.5
Number of DBA cells	30
Number of 8.6 m straights	15
Beta-functions in the center of the 8.6 m straights: $\beta_x, \beta_y$ [m]	18, 3.1
Number of 6.6 m straights	15
Beta-functions in the center of the 6.6 m straights: $\beta_x, \beta_y$ [m]	1.5, 0.8
Number of dipoles	60
Circulating current at 3 GeV, multi-bunch [mA]	500
Radio frequency [MHz]	499.68
Harmonic number	1320
Number of bunches at 80% fill	1056
Nominal bending field at 3 GeV [T]	0.4
Dipole critical energy at 3 GeV [keV]	2.4
Total Bending magnet radiation energy loss [keV]	286.4
Radiation energy loss per damping wiggler [keV]	129.3
Vertical emittance [nm-rad]	0.008
Horizontal emittance of bare lattice [nm-rad]	2.1
Horizontal emittance with three 7 m 1.8 T damping wigglers [nm-rad]	0.9
Horizontal emittance with eight 7 m 1.8 T damping wigglers [nm-rad]	0.55
Momentum compaction factor	$3.7 \times 10^{-4}$
Bunch length, RMS, natural [mm, ps]	2.9, 10
Energy spread, RMS	0.05 – 0.1%

**Table 2. Electron Beam Size and Divergence of NSLS-II sources.**

Type of source	Low- $\beta$ straight section (6.6m)	High- $\beta$ straight section (8.6m)	0.4T Bend magnet	1T three-pole wiggler
$\sigma_h$ [ $\mu\text{m}$ ]	28.	99.	44.2 (35.4-122)	136
$\sigma_h'$ [ $\mu\text{rad}$ ]	19.	5.5	63.1 (28.9 – 101)	14.0
$\sigma_v$ [ $\mu\text{m}$ ]	2.6	5.5	15.7	15.7
$\sigma_v'$ [ $\mu\text{rad}$ ]	3.2	1.8	0.63	0.62

**Table 3. Electron Beam Size and Divergence of NSLS sources.**

Type of source	Straight section	Bend magnet
$\sigma_h$ [ $\mu\text{m}$ ]	307	260 - 464
$\sigma_h'$ [ $\mu\text{rad}$ ]	231	261 - 352
$\sigma_v$ [ $\mu\text{m}$ ]	11	62 - 90
$\sigma_v'$ [ $\mu\text{rad}$ ]	32	13.5 – 14.1

**Table 4. Basic Parameters of NSLS-II Radiation Sources.**

<b>Name</b>	<b>U14</b>	<b>U19</b>	<b>EPU45</b>	<b>EPU100</b>	<b>DW100</b>	<b>SCW60</b>	<b>Bend</b>	<b>3PW</b>
<b>Type</b>	SCU	CPMU	EPU	EPU	PMW	SCW	0.4T bend magnet	1T three-pole wiggler
<b>Photon energy range</b>	Hard x-ray (1.8 - 30 keV)	Hard x-ray (1.5 - 20 keV)	Soft x-ray (180 eV - 7 keV)	VUV (8 eV - 4 keV)	Broad band (<10 eV - 100 keV)	Very hard x-ray (<10 eV - 200 keV)	Soft and tender x-ray (<10 eV - 12 keV)	Hard x-ray (0.1 - 30 keV)
<b>Period (mm)</b>	14	19	45	100	100	60		
<b>Length (m)</b>	2.00	3.00	4.00	4.00	7.00	1.00		
<b>No. of Periods</b>	143	158	89	40	70	17		
<b>Peak magnetic field strength B(T), linear mode</b>	1.68	1.14	1.03	1.5	1.8	6.00	0.4	1.0
<b>Max <math>K_v</math>, linear mode</b>	2.20	2.03	4.33	14.01	16.81	33.62		
<b>Peak magnetic field strength B(T), circular mode</b>			0.64	1.15				
<b>Max <math>K_h=K_v</math>, circular mode</b>			2.69	10.74				
<b>Minimum hv fundamental, linear mode (eV)</b>	1789	1470	183	8.6				
<b>Minimum hv fundamental, circular mode (eV)</b>			411	14.6				
<b>hv critical (keV)</b>					10.77	35.91	2.39	5.99
<b>Total power (kW)</b>	16.08	11.18	12.09	25.64	64.60	102.55		
<b>Horizontal angular power density (kW/mrad)</b>							0.0228	0.0570
<b>On-axis power density (kW/mrad<sup>2</sup>)</b>	103.70	77.86	40.03	26.33	55.30	43.90	0.0879	0.2197

## Brightness

For many experiments, especially those involving imaging or microscopy, where the beam must be focused down to a small spot, the key figure of merit of user radiation sources is their time average brightness. This is the flux output per unit bandwidth, per unit source area, and per unit solid angular divergence. Undulators and wigglers are excellent sources of high brightness radiation. The brightness of the base set of radiation sources for NSLS-II is shown in Figure 1. For the undulators, the tuning curves of harmonics 1, 3, 5, 7, and 9 are shown. These tuning curves show the variation of the peak brightness of the undulator harmonics as the magnetic field strength, and hence K parameter, is varied from  $K_{\max}$ , listed for each undulator in Table 4, down to  $K_{\min} \sim 0.4$ .

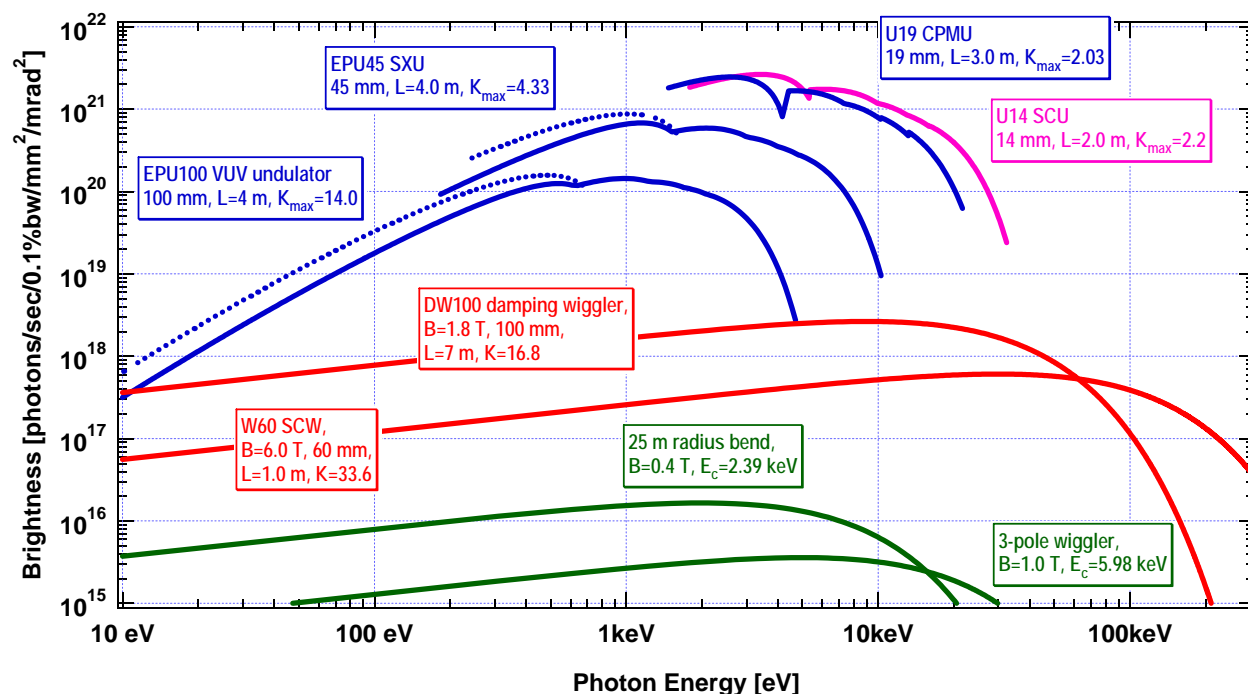


**Figure 1. Brightness vs. photon energy for various devices at NSLS-II.**

The brightness of the U14 and U19 hard x-ray undulators is the highest of any devices planned for NSLS-II. This is due in part to the short period of these devices, thereby increasing the number of periods contributing to the flux output, and in part to the short output wavelengths compared to the soft x-ray (EPU45) and VUV (EPU100) undulators. For diffraction-limited undulator radiation, which characterizes a good portion of the range of these four undulators, the brightness varies inversely as the square of the output wavelength. Note that the brightness of the hard x-ray undulators (U14 and U19) exceeds the  $10^{21}$  ph/s/0.1%BW/mm<sup>2</sup>/mrad<sup>2</sup> level.

The wigglers provide broadband, high brightness sources of x-ray radiation. Each of the wigglers covers nearly the entire photon energy range. The superconducting wiggler SCW60 is optimized for very high-energy x-ray work (i.e., above  $\sim 60$  keV), while the damping wiggler DW100 is a high-flux, hard x-ray source with smooth spectral output extending down through the soft x-ray and VUV photon energy ranges. Figure 1 shows the brightness of the EPU45 and EPU100 elliptically-polarized undulators in two polarization modes: helical (or circular), shown as dotted lines, and linear, shown as solid lines. The circular polarized mode has intensity only in the fundamental and is slightly brighter than the linearly

polarized mode at the same energy. It is expected that this mode will be used for all work below 2 keV for the EPU45 and below 850 eV for the EPU100, unless linearly polarized light is specifically required.

NSLS-II bending magnets will be bright sources which extend from the infrared to the hard x-ray. These sources will be useful up to a few times the critical energy of 2.39 keV, i.e., up to ~10 keV. The bending magnet brightness peaks at ~2 keV, making it an ideal broadband source in the soft x-ray (0.1–2 keV) and low-energy x-ray (2–5 keV) ranges.

The 3-pole wiggler (3PW) source have a critical energy of 6 keV, making them very useful continuum hard x-ray sources up to ~25 keV. The emitted horizontal fan from these devices is 2 mrad wide.

## Flux

For those experiments which do not require a very collimated and/or focused beam, the photon spectral flux is the key figure of merit. This is the number of photons per unit bandwidth per unit time. Figure 2 below shows the flux for the NSLS-II radiation sources. For both wigglers and bend magnets, a horizontal collection of 1 mrad is shown.

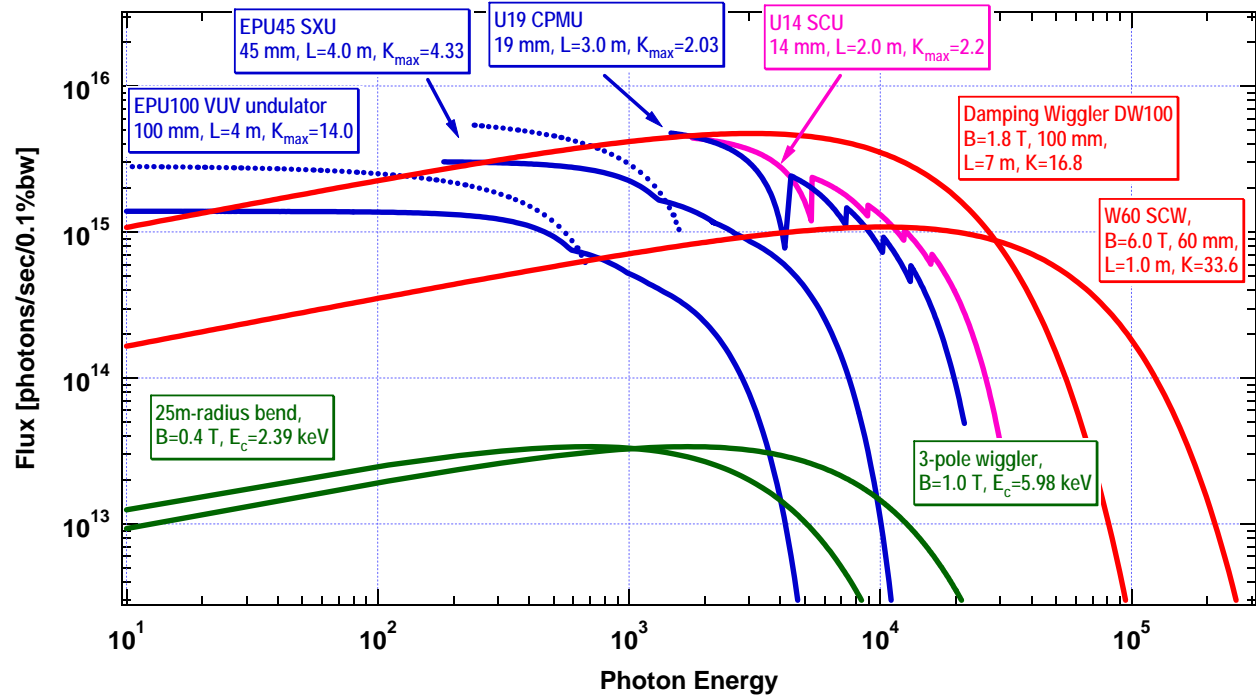


Figure 2. Flux vs. photon energy for various devices at NSLS-II.

Figures 3 and 4 show the comparison of the above NSLS-II devices with the existing NSLS sources.

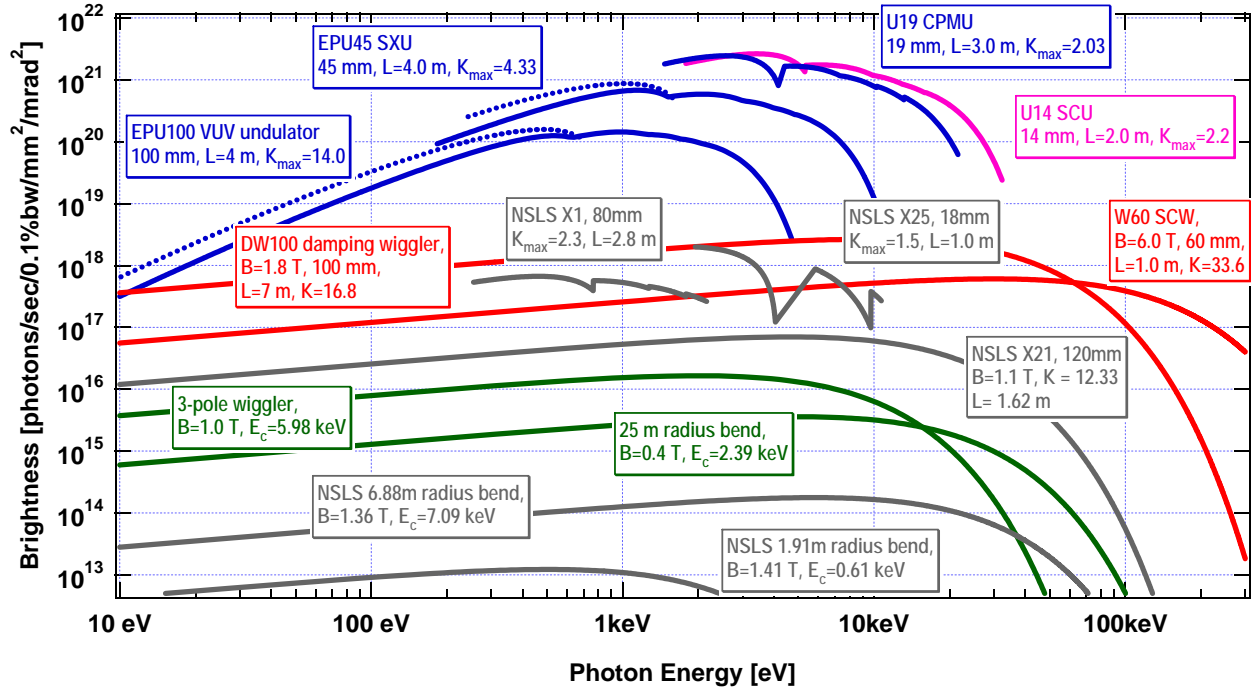


Figure 3. Brightness comparison for NSLS-II and NSLS sources.

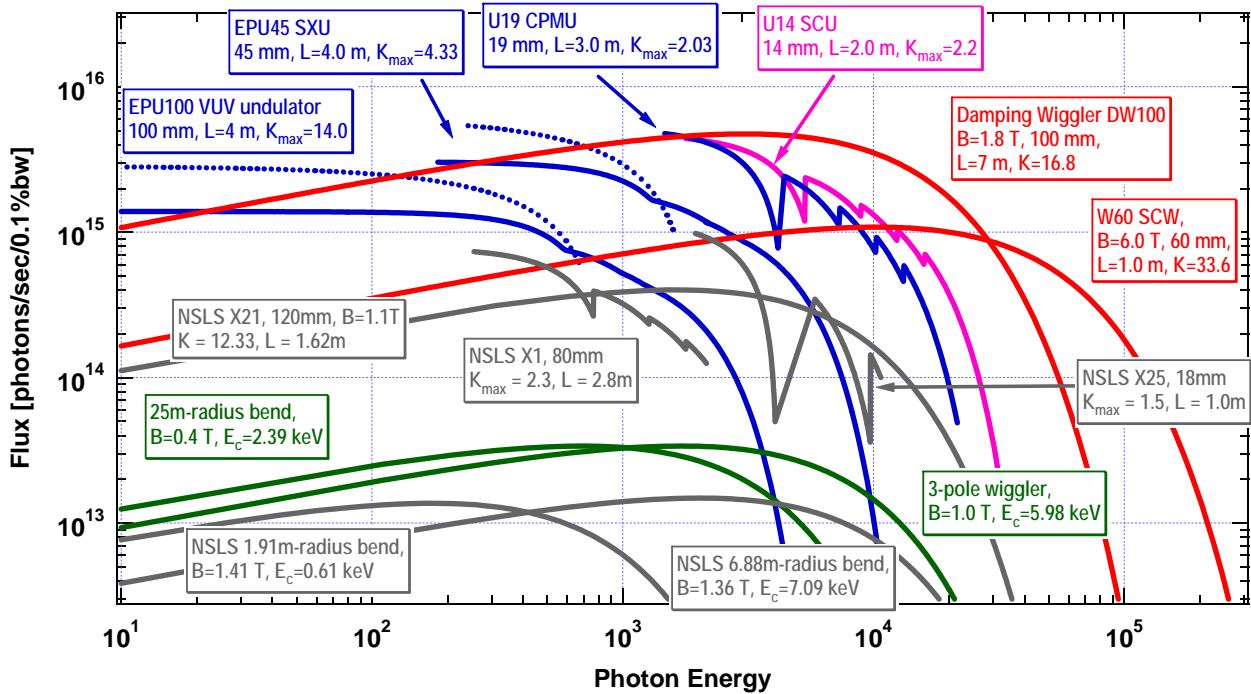
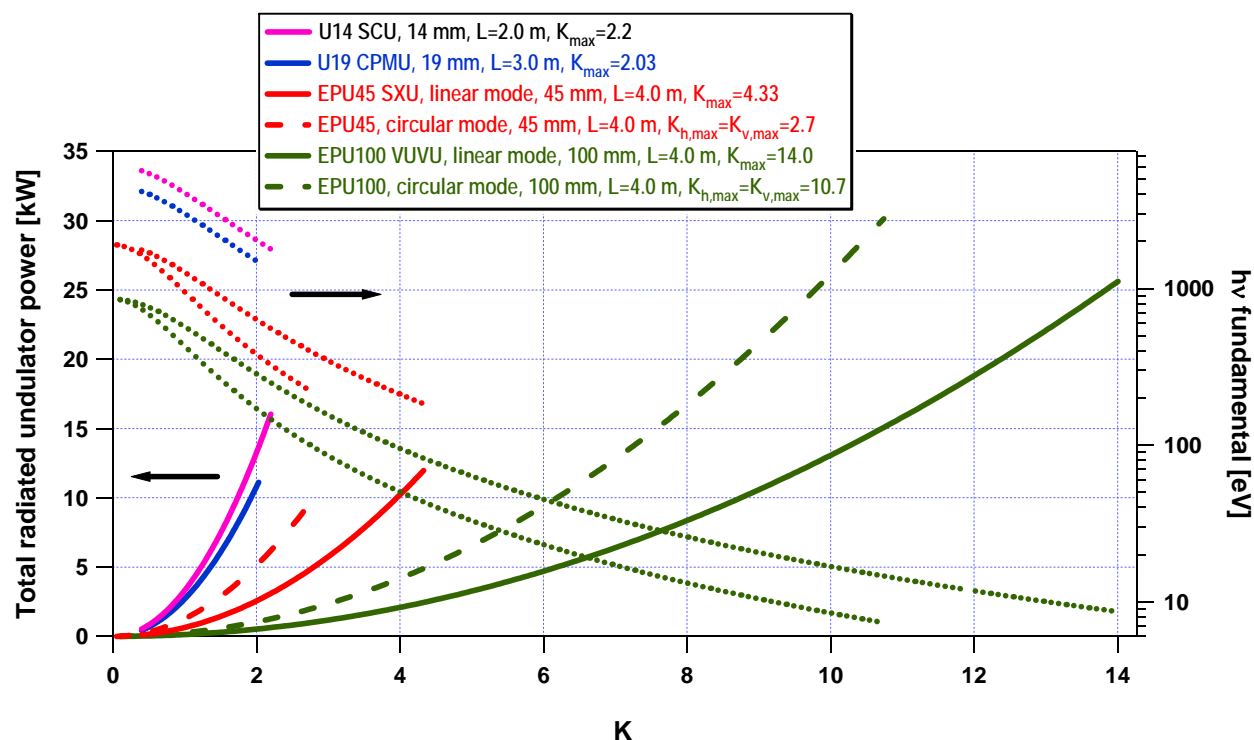


Figure 4. Flux comparison for NSLS-II and NSLS sources.

## Power

Table 4 gives the maximum total output power of the NSLS-II radiation sources. Figure 5 shows how the total output power of the undulators varies as their K value is changed from  $K_{\min}$  (taken to be  $\sim 0.4$ ) to  $K_{\max}$ , as given in Table 4. For reference, the corresponding photon energy of the undulator fundamental as a function of K is also shown on the right axis. The photon energy of harmonic  $n$  is  $n$  times that of the fundamental.

The total power radiated by the undulators at their maximum K settings (i.e., at minimum magnetic gap) is in the 10–30 kW range. The total power output from the NSLS-II wigglers is higher than that of the undulators, at nearly 65 kW, while that of the NSLS-II bend magnets and 3-pole wigglers is very much less, at only  $\sim 23$  W and  $\sim 57$  W per horizontal mrad, respectively.



**Figure 5. Total output power of the NSLS-II undulators as a function of the undulator parameter, K.**

## Power density

Table 4 also gives the maximum (on-axis) angular power density of the NSLS-II radiation sources. Figure 6 shows how the maximum angular power density of the undulators varies as their K value changes from  $K_{\min}$  (taken to be  $\sim 0.4$ ) to  $K_{\max}$ , as given in Table 4. For reference, the corresponding energy of the photons radiated in the fundamental as a function of K is also given. The maximum undulator angular power density radiated by the undulators at their maximum K settings (i.e., at minimum magnetic gap) varies from 25 to 100 kW/mrad<sup>2</sup>. The wiggler angular power density output is in the 25–55 kW/mrad<sup>2</sup> range, while the bend magnet and 3-pole wiggler values are again very much less, at 88 W/mrad<sup>2</sup> and 220 W/mrad<sup>2</sup>, respectively. The angular power density figure also shows that the output angular power density of the EPU in circular polarization mode is much lower than in linear polarization mode, and has a different dependence on K. This is primarily because in circular mode there are no higher harmonics, just the fundamental. An advantage of the circular polarization mode is the lower output

power density, which simplifies the design and operation of high energy-resolution beamlines by reducing the thermal deformations of the optical elements.

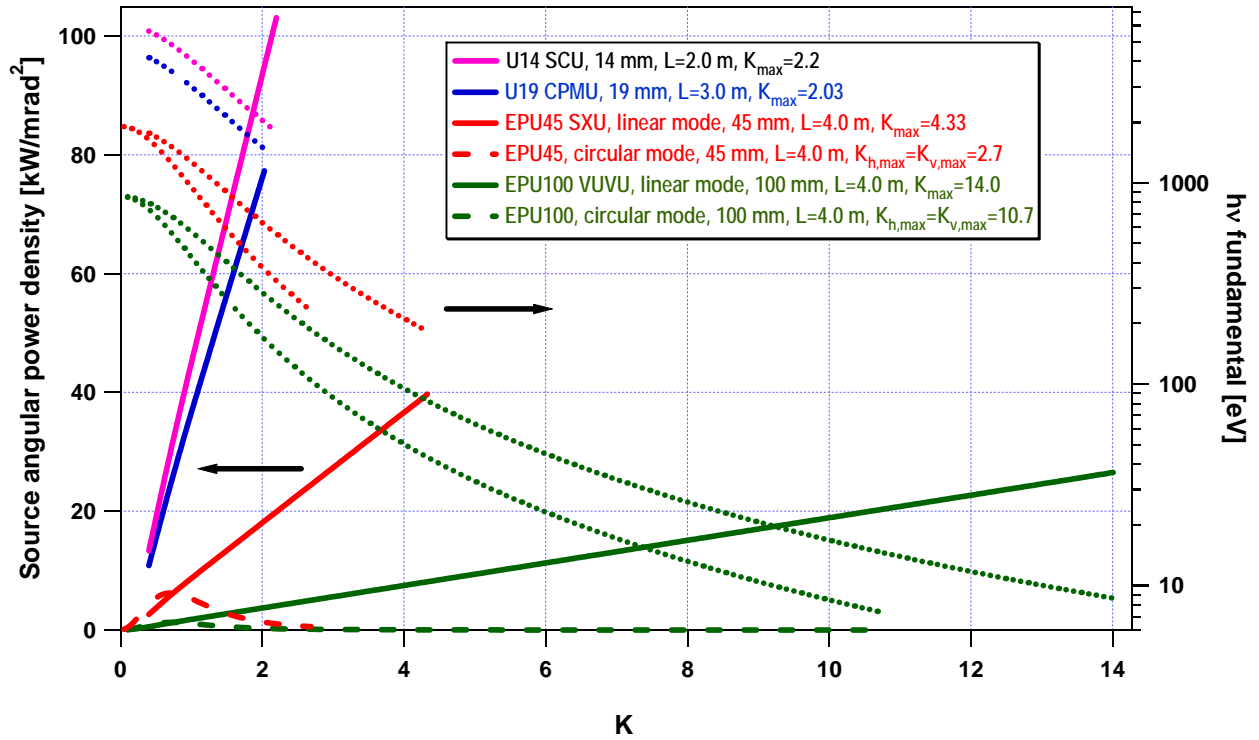
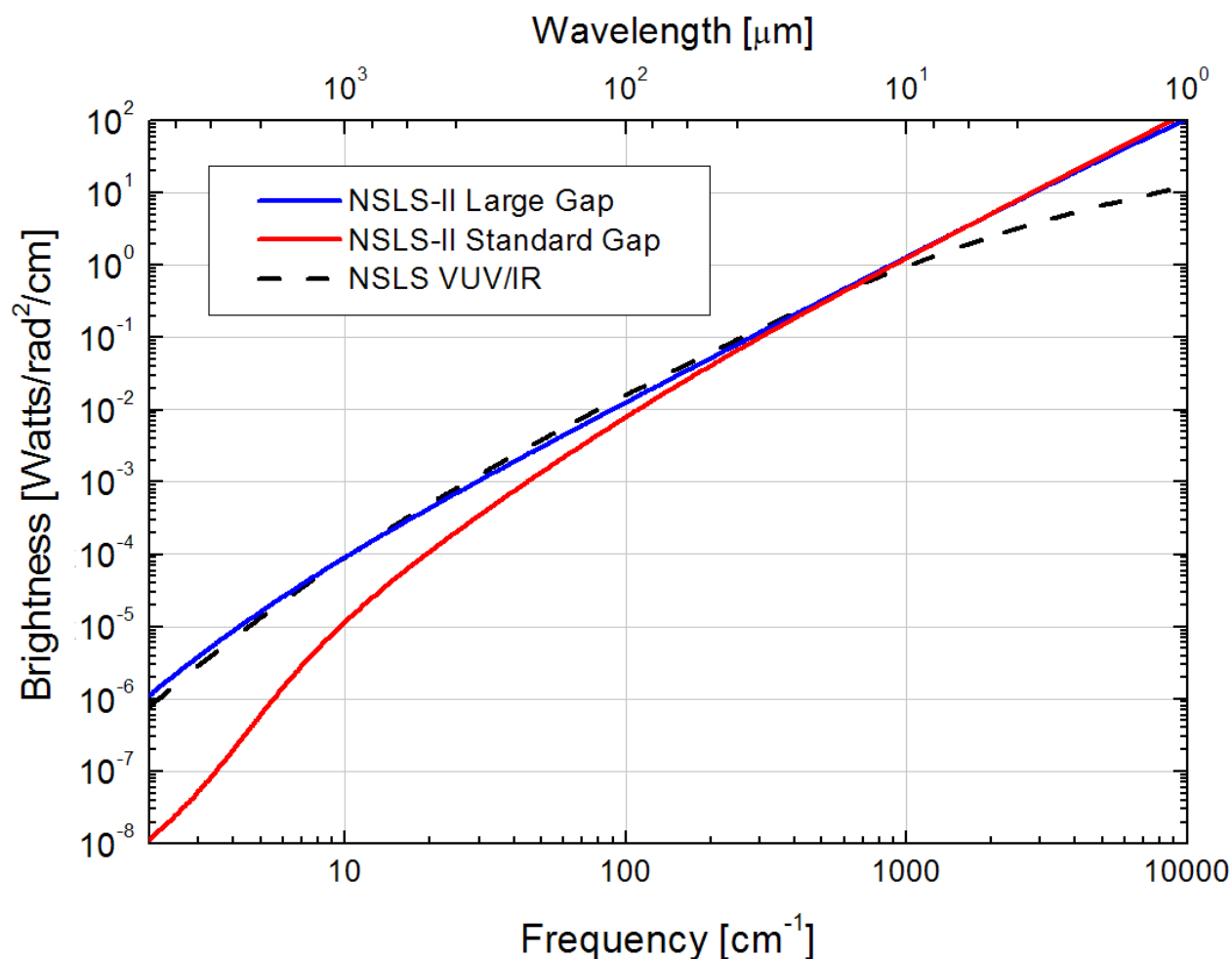


Figure 6. Angular power density of the NSLS-II undulators as a function of the undulator parameter, K.

### Infrared sources

Figure 7 shows the NSLS-II brightness for the very far-, far- and mid-infrared spectral ranges, for both the standard gap and large gap (90 mm) dipoles and associated extraction chambers. The brightness curves are compared to that of the existing VUV/IR ring. In the mid-infrared range from 1 to 20 micron wavelengths, the standard-gap dipole and extraction optics are sufficient. In this range, the lower emittance of NSLS-II results in up to an order of magnitude greater brightness compared to NSLS. In the very far-infrared range, especially for wavelengths greater than 1 mm, the large-gap dipole and extraction optics become essential in preserving brightness, and can be seen to produce spectral brightness equal to the world class performance of the NSLS very far-IR ports. In this wavelength range, the standard-gap dipole and extraction suffers both from waveguide cutoff effects and limitations from small horizontal collection fan angle.





**Figure 7. NSLS-II brightness in the infrared range.**

### **Distribution of sources available for user beamlines**

NSLS-II will accommodate at least 58 beamlines for user experiments, distributed by type of source as follows:

- 15 low-beta ID straights for user undulators or superconducting wigglers
- 4 high-beta ID straights for user undulators
- 8 high-beta straights for user damping wigglers
- 27 BM ports providing broadband sources covering the IR, VUV, and soft x-ray ranges. Any of these ports can alternatively be replaced by a 3-pole wiggler port covering the hard x-ray range.
- 4 BM ports on large gap (90 mm) dipoles for very far-IR

If multiple (probably two) IDs, canted in horizontal angle, are installed in each straight section, the maximum number of ID ports doubles from 27 (15+4+8) to 54. In addition, multiple endstations and/or multiple hutches per beamline are also possible.

## Floor layout

The standard floor space available for beamline components, ranging from just outside the ring shield wall to the exterior walkway, is given in Table 5 below. Note that these dimensions vary depending on type of source and type of cell (high- $\beta$  or high- $\beta$  ID straight). Non-standard locations for beamline components, either inside the shield wall or extension beyond the exterior walkway for extra long beamlines, can also be considered.

**Table 5. Floor Layout Dimensions for Beamlines.**

<b>Source description</b>	<b>Distance from source point to downstream face of shield wall</b>	<b>Distance from source point to walkway</b>
High- $\beta$ ID straight	27.9 m	67.1 m
Low- $\beta$ ID straight	26.7 m	66.8 m
3PW downstream of high- $\beta$ ID	21.9 m	62.8 m
3PW downstream of low- $\beta$ ID	22.8 m	64.2 m
Bend downstream of high- $\beta$ ID	21.2 m	63.8 m
Bend downstream of low- $\beta$ ID	22.1 m	65.2 m